Improving Influx Constant and Ratio Estimation in FDOPA Brain PET Analysis for Parkinson's Disease

Xiao-Bo Pan, PhD[1]; Thomas G. Wright, PhD[1]; F. Joel Leong, MD, PhD[2]; Robert A. McLaughlin, PhD[1]; Jérôme M. Declerck, PhD[1]; and Daniel H.S. Silverman, MD, PhD[2]

[1]*Siemens Molecular Imaging, Oxford, United Kingdom; and* [2]*Department of Molecular and Medical Pharmacology, David Geffen School of Medicine, UCLA, Los Angeles, California*

PET studies using L-3,4-dihydroxy-6-^{18}F-fluorophenylalanine have been applied to assess the diminished functionality of the striatum in patients with suspected Parkinson's disease. Two techniques for analyzing such studies are ratio methods and graphically computed influx constants. We propose a method for improving the consistency with which scans obtained by either of these techniques are analyzed. The method is based on a fully 3-dimensional analysis of the images. **Methods:** Fifty-one dynamically acquired datasets were corrected for motion before analysis. Regions of interest (ROIs) for the analysis were determined by manual affine registration to a standard template, using a separate transformation for each ROI. Indicator values for each ROI were computed by averaging the values of voxels having the highest activity within a specified proportion of the voxels in the ROI, to increase the robustness to perturbations in the ROI position. Sensitivity was analyzed by examining the variation in results obtained when the ROIs were translated by up to 6 mm. **Results:** We observed significant percentage differences in the computed influx constant before and after motion correction (mean variation ± SD, −0.75% ± 9.5% averaged over all regions of all patients). Our method was robust to placement of the cerebellum ROI, whereas a 2-dimensional analysis based on hand-drawn ROIs was associated with a 2- to 3-fold greater percentage variation in uptake for translations of 2 mm or more in ROI position. When we compared the 2 quantification techniques, our influx constants and ratios correlated at $r^2 = 0.91$, $P < 0.0001$. **Conclusion:** Motion correction is an important step for computing reliable results in dynamic studies. The robustness of the results can be increased further by using standard normalized volumetric ROIs and by using the average value of a specified proportion of the voxels with the highest activity in the ROI as an indicator for that ROI. Influx constant values computed using our analysis technique closely correlated to values computed with ratio methods using this general approach.

Received Mar. 30, 2005; revision accepted Jul. 11, 2005.

For correspondence or reprints contact: F. Joel Leong, MD, PhD, UCLA Department of Molecular and Medical Pharmacology, CHS 23-120, MC 173517, 10833 Le Conte Ave., Los Angeles, CA 90095.

E-mail: jleong@mednet.ucla.edu

Guest Editor: Wolf-Dieter Heiss, MD.

Key Words: FDOPA; Patlak graphical analysis; ratio method; Parkinson's disease; PET

J Nucl Med 2005; 46:1737–1744

Idiopathic Parkinson's disease (PD) is a progressive degenerative motor disorder characterized classically by a distinct constellation of physical signs (tremor, bradykinesia, rigidity). Diagnoses based on clinical examination, however, can be inaccurate in up to 25% of patients (*1,2*). A variety of biomarkers have been used to image the nigrostriatal dopaminergic system (*3,4*), such as L-3,4-dihydroxy-6-^{18}F-fluorophenylalanine (FDOPA) used in conjunction with PET. In PD and other parkinsonian syndromes, the degeneration of the substantia nigra is manifested as diminished uptake of FDOPA in the corpus striatum.

FDOPA uptake can be quantified by ratio methods (e.g., the ratio of the striatum to the cerebellum or of the striatum to the occipital lobe) (*5–7*), graphical method (influx constant, K_i) (*8–10*), or compartmental models (*11–13*), although the last are less frequently used in practice because of their additional complexity. In this paper, we analyze some of the factors that influence results obtained by the first 2 methods—for example, patient movement during scanning, the shape and placement of regions of interest (ROIs), and the heterogeneous nature of voxel intensities within the ROIs. We propose a method for estimating the influx constant in a consistent way that includes motion correction, affine registration (allowing translation, rotation, scaling, and shearing in each dimension of the image independently) for standard ROI delineation, and extraction of an ROI indicator value from a proportion of the voxels with the highest uptake values. The robustness of this method was investigated, and its results were correlated with those of the ratio method.

Kinetic Modeling of FDOPA

FDOPA is a tracer used in PET studies for assessing dopamine system dysfunction linked with PD and other

parkinsonian syndromes. FDOPA targets a dopamine synthetic enzyme, aromatic amino acid decarboxylase, in the presynaptic process. Aromatic amino acid decarboxylase is present in the dopaminergic, noradrenergic, and serotonergic systems but is contained primarily within dopaminergic neurons. It converts FDOPA to ^{18}F-fluorodopamine, which is then stored in dopaminergic neurons. The extent of ^{18}F-fluorodopamine accumulation then provides an estimate of the dopamine synthesis capacity of that region. However, this measure cannot differentiate between changes occurring in activity per neuron terminal and changes in the total number of terminals. It represents a product of average activity per neuron and the number of terminals in the ROI (*14*).

Patlak Graphical Analysis

FDOPA uptake can be quantified by K_i, which is the slope of a linear fitting between 2 time–activity curves: the time–activity curve of the ROI $C_{striatum}(t)$ and the time–activity curve of the blood input function $C_{blood}(t)$. In FDOPA studies, the blood input function can be replaced by the time–activity curve of a nonspecific reference region, such as the cerebellum $C_{cerebellum}(t)$ or occipital cortex $C_{occiptal}(t)$ (*6*). $K_i^{cerebellum}$ (using the cerebellum as reference region) is derived in this study according to the following equation (*9*):

$$\frac{C_{striatum}(t)}{C_{cerebellum}(t)} = V_0 + K_i \frac{\int_0^t C_{cerebellum}(s)ds}{C_{cerebellum}(t)},$$

where V_0 is the initial volume of distribution. The fact that the time–activity curve is obtained from the same voxel or ROI in each frame of a dynamic scan assumes that the patient is stationary during the scan; in practice, some patient movement is unavoidable. One aim of this study was to develop a motion-correction strategy and hence to investigate the extent of patient movement during a scan and the consequent effect on the estimated influx constant.

$K_i^{cerebellum}$ (K_i^c) can be obtained either in a user-defined ROI (*6*) or at every voxel, such as with statistical parametric mapping analysis (*15*). In this paper, we focus on the more commonly used ROI-derived influx constant. Because of the relatively small size of striatal structures, partial-volume effects and inaccurate definition of ROIs can affect the accuracy and reliability of the estimated influx constant (*16*). A preliminary study of influx constant sensitivity to the shape and placement of the ROI was conducted using manually drawn ROIs on a single axial slice of the image. The influx constant was found to vary from around 4% to 29% with 1- to 4-voxel ROI movement within the slice (voxel resolution, 1.47 mm). The variation between slices was 5%–10%, although a variation of less than 5% could be achieved by repositioning the ROI on every slice. These results reflect the importance of defining a standard ROI and a systematic way of positioning it in order to achieve a consistent influx constant. To date, several different strategies have been used for ROI placement. In one paper, standard elliptic ROIs were placed on a mean image of 4 central slices (thickness, 17 mm) (*6*). Other ROI methods have included defining standard volumes on summed images (where a subset of the frames are averaged together) or placing regions on PET images coregistered to individual MR images (*15*). Here, we propose a 3-dimensional volume-of-interest method that uses affine registration to a standard brain template, and we investigate its robustness.

Static Ratio Analysis

The ratio method does not require dynamic scans. It uses a single static scan (duration, 10–30 min) obtained at some time (45–125 min) after the injection of radiotracer, and the ratio is defined over values of the ROI and a reference region. For example:

$$R_{s\text{-}to\text{-}c} = ROI_{striatum}/ROI_{cerebellum}.$$

Motion correction as described in the previous section is not applicable to the ratio method because only a single scan is considered (although patient movement during the acquisition will obviously affect scan quality by introducing blurring). However, the definition of the ROI and the start time and duration of the scan will affect the consistency and reproducibility of the values produced by this method.

MATERIALS AND METHODS

Dynamically acquired FDOPA PET scans of 51 patients (33 men and 18 women; mean age ± SD, 56 ± 14 y) were analyzed. Scans were acquired using a high-resolution full-ring scanner (ECAT HR+; Siemens/CTI) in 3-dimensional mode, with 63 contiguous slices acquired simultaneously. Slice thickness was 2.4 mm, and reconstructed resolutions were 6–7 mm in full width at half maximum. Each scan consisted of 18 frames covering a total acquisition time of 125 min, starting immediately after injection (the acquisition began with 6 frames of 30 s each, followed by 4 of 3 min, 5 of 10 min, and finally 3 of 20 min). When performing our Patlak graphical analysis, we used frames 12–18 (25–125 min) for computation of K_i^c and data from all frames for calculation of the input time–activity curve. Two of the 51 patients were excluded from the study after preliminary experiments found that, for unknown reasons, their cerebellar uptake was slower than that of all other patients by more than a factor of 2.

Motion Correction

Patient movement of more than 1 cm during the acquisition took place in several studies. To mitigate the effects of this movement, we corrected the scans for patient motion. A strategy for motion correction of frames taken during a dynamic acquisition has been described (*17*). By supersampling the source volume to an intermediate geometry before registration, this strategy reduces the inherent bias of registration schemes to favor the identity transformation when 2 similar images are registered with the same geometry. We started from the end of the study rather than the beginning because of the better image quality of later frames.

First, we initialized the combined transformation matrix T to the identity. For frames $f = 17, 16, \ldots, 7$ we resampled frame

($f + 1$) to the intermediate geometry, registered (rigidly, using translation and rotation) frame f to this resampled frame, postmultiplied the combined transformation matrix T by the transformation matrix for this registration result, and resampled the registered frame f into the original geometry of the final frame 18 using the updated combined transformation matrix T.

For $f = 6, \ldots, 1$ we resampled frame f into the original geometry of the final frame 18 using the combined transformation matrix T calculated as above.

No motion correction was performed on the 30-s frames acquired during the first 3 min of acquisition because of their poor image quality and the subsequent risk of misregistration. Because of their short duration, it is reasonable to expect any movement to be minimal in these frames, and hence we use the transformation obtained for frame 7 to align these scans.

Any voxels that were not present in all frames (because of spatial transformation) were set to the background value in all frames, to ensure that voxels being considered for the analysis had valid values throughout the scan. After motion correction, all 49 datasets were verified visually, checking alignment of the scalp and, where visible, alignment of the striata to ensure that the motion correction had been performed successfully (the criterion used was that the movement of the scalp was less than half the thickness of the scalp over the entire study).

Standard ROIs

We next located the ROIs. The regions specified were the left and right striatum and the cerebellum, which was used as the reference region. We segmented these fully in 3 dimensions (*15*), using manual affine registration to the automated anatomic labeling (AAL) standard brain template (*18*). However, because affine registration is not generally sufficiently accurate to simultaneously register both the striata and the cerebellum to the AAL template for any particular patient (locally deformable registration is usually needed to achieve this accuracy), we obtained each region using a separate affine transformation. Clearly, care must be taken to ensure that transformations that affect volume have a consistent effect over all 3 regions, because the volumes of the striata and the cerebellum are nearly proportional to total brain volume and to each other (*19*).

The visual guides used during the registration included the brain outline, the left and right caudate regions, the left and right striatal regions, and the cerebellum (Fig. 1). The images registered were the final frame of the dynamic study and the standard brain template, although other frames would also be suitable.

Coarse alignment of the brain included translating the brain so that it is centered within the cortical boundary; rotating around the center of the boundary between right caudate and right putamen to coarsely align the lower boundary of the brain, as appears in the template; and uniformly scaling the brain so that the cortex fits within the brain boundary. Minor corrections for overall alignment of the right striatum included shifting and rotating the brain as necessary to align the main structures, using the cerebellum and the boundary between the right caudate and right putamen as landmarks for matching to the standard template, and fixing the scaling when necessary. Completing alignment of the right striatum included using minor translations as necessary to ensure that the caudate was visible in all slices and that the boundary between right caudate and right putamen matched the standard template. The scale and shear parameters were not changed afterward. The transformation for the right striatum was recorded at that point.

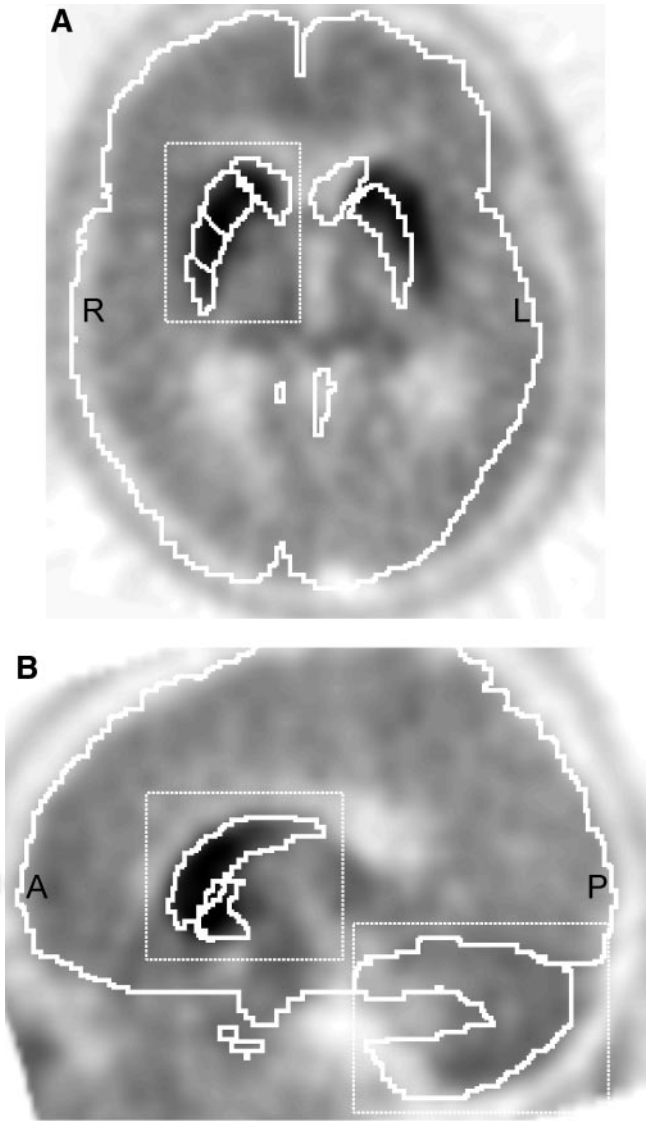

FIGURE 1. Registered images with subputamen ROIs. (A) Right striatum registered to AAL template (single axial slice; registered region highlighted). Note that a new transformation will be needed to register the left striatum. (B) Cerebellum and left striatum registered to AAL template (single sagittal slice).

Completing alignment of the left striatum was performed as for alignment of the right striatum, using translation only. The transformation for the left striatum was recorded at that point. Completing alignment of the cerebellum was performed as for alignment of the right striatum, using translation only. The transformation for the cerebellum was recorded at that point.

Using the AAL template as a reference, we extracted voxels from within the following 5 regions: cerebellum, left and right caudate, and left and right putamen.

Early PD is associated with effects on the caudal putamen, and then the rostral putamen is affected as the disease progresses (*20*). To assess these effects, we subdivided each putamen into 3 regions of roughly equal volume along its length by using 2 spheres centered on the heads of the caudate nuclei with radii of 16 and 27 mm (chosen to give us equality of volume between the 3 divisions of the putamen). Thus, for each patient we defined 8 regions for

quantification of FDOPA uptake (left and right caudate and 3 putamen regions on each side) and 1 reference region (cerebellum).

Sensitivity of Influx Constant and Ratio Values to ROI Position

Once the ROIs had been positioned, we conducted a sensitivity analysis of the influx constants and ratios with respect to placement of the ROIs. Translations of ±2 and ±4 mm were applied to ROIs in the left-right (L-R), anterior-posterior (A-P), and superior-inferior (S-I) directions (treating each direction separately) to simulate potential variation of ROI positions in the manual affine registration process (an additional translation of ±6 mm was applied to the cerebellum ROI because it is larger and hence potentially liable to greater misalignment). First, only the cerebellum ROI was translated, maintaining a fixed position for the striatum ROIs. Subsequently, the cerebellum ROI was maintained in a fixed position, whereas the positions of the striatum ROIs were perturbed. The average percentage variation in K_i^c and ratio ($R_{s\text{-}to\text{-}c}$) values was then calculated for the 49 patients.

To allow a direct comparison with our preliminary 2-dimensional study of sensitivity using manually drawn ROIs on a single slice, we computed the average percentage variation in the L-R and A-P directions for all combinations of ±2- and ±4-mm translations. This computation gave values for translations of up to $\sqrt{(4^2 + 4^2)} \approx 5.9$ mm for the diagonal displacement.

Calculation of ROI Indicator Value

Because of the effect of partial volumes (*21*) and different disease states, the contents in any ROI may be heterogeneous. A common method to obtain a representative intensity value is to compute the mean value of voxels in the ROI, but this method may potentially include substantial background noise. Additionally, a problem that we observed when fitting the cerebellum to the AAL template was that the functional region visible in the PET scan was significantly smaller than the anatomic region of the template. To overcome such problems, a percentage thresholding method was proposed by Rottenberg et al. (*22*) to extract a value from each ROI. That method uses the average value of the voxels whose intensity is above 85% of the maximum intensity within the ROI. However, depending on the distribution of activity within the ROI, the actual number of voxels to be averaged could vary substantially, biasing analysis toward the healthy part of the ROI without consideration of its volume. To alleviate this difficulty, we propose computing the mean of a fixed volume within the ROI, where the volume comprises only the brightest pixels within the ROI. We expect that this method will reduce the partial-volume effect and therefore increase the sensitivity and allow more tolerance to misalignment of ROIs.

For the graphical Patlak analysis, the voxels with greatest activity are determined from the average of frames 4 through 18, omitting the first 3 frames because of their high level of noise. For the static analysis, voxels are selected from the static scan under consideration. Because of this difference between the dynamic and static analyses, slightly different subsets of the ROI voxels may be used in the computations.

Comparison of Ratios and Influx Constants

Ratios will vary slightly depending on which late frame is used in the computations. To account for this variation, we computed $R_{s\text{-}to\text{-}c}$ values using 4 different static frames: the final frame in our acquisition, the penultimate frame, the average of the final 2 frames (i.e., acquisition from 85 to 125 min), and the average of the final 3 frames (i.e., acquisition from 65 to 125 min). The results from each were compared with K_i^c values, and the correlation was computed using standard Pearson correlation coefficients. A sensitivity analysis was also performed using different proportions of the brightest voxels from the cerebellum (25%, 50%, 75%, and 100%) and different proportions for the striatum regions (10%, 20%, . . . , 100%). For each proportion, the degree of correlation between $R_{s\text{-}to\text{-}c}$ and K_i^c was recorded.

RESULTS

Motion Correction

After correction, no significant motion was observed between corrected frames for any of the patients (for almost all patients there was no visible motion). Slight motion (approximately half the visible thickness of the scalp) was visible for 1 patient during the first 6 (uncorrected) frames, although this motion was still within our criterion.

In assessing the effects of motion correction on the results, we considered the amount of motion present, in particular the maximum and average translations and rotations (about the center of the image) across all frames (Fig. 2).

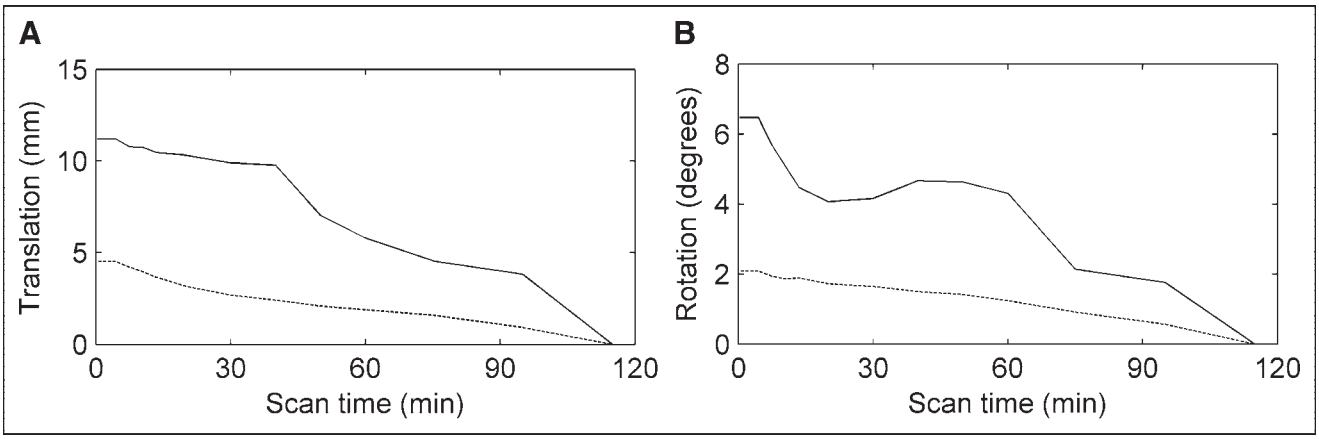

FIGURE 2. Average (dashed line) and maximum (solid line) translation (A) and rotation (B) over all 49 datasets against scan time.

TABLE 1
Average Percentage Variation in Influx Constant and Ratio Values Across All 8 Values of All 49 Cases with Varying Cerebellum ROI Position

	Shift (mm)					
	±2		±4		±6	
Direction	K_i^c	$R_{s\text{-}to\text{-}c}$	K_i^c	$R_{s\text{-}to\text{-}c}$	K_i^c	$R_{s\text{-}to\text{-}c}$
L-R	0.15	0.13	0.32	0.26	0.52	0.43
A-P	0.29	0.42	0.61	0.79	0.97	1.11
S-I	0.63	0.80	1.53	1.92	3.0	3.43

The horizontal portion of the curves during the first 3 min corresponds to those frames on which we did no additional motion correction. The earliest frames typically required large transformations—not surprising, because frames are registered to the final frame.

The next effect we considered was the impact of motion correction on K_i^c values. Across all 8 regions and 49 patients (i.e., 392 values in all), the percentage variation in K_i^c ranged from −37% to 60%, with a mean of −0.75% and an SD of 9.5%. For this experiment, calculations were made using 50% of the brightest voxels from the cerebellum and 40% of the brightest voxels from each striatum region.

Sensitivity of Influx Constants and Ratios to ROI Position

The effect of applying small translations to the cerebellum ROI is summarized in Table 1, and the results of translating the striatum ROIs are recorded in Table 2. These experiments were performed using 50% of the brightest voxels from the cerebellum and 40% of the brightest voxels from each striatum region.

To compare the percentage variation of K_i^c and the ratio values to the influx constant obtained from our preliminary study in 2 dimensions using a manually drawn ROI, we plotted ROI translation against percentage variation in the value (Fig. 3). The percentage variations from both in-slice directions, L-R and A-P, were averaged to produce the data for this plot, as well as data taken from the combination of L-R and A-P translations simultaneously. The 2-dimensional results were obtained using a range of translations of 1–4 voxels with a voxel size of 1.47 mm. The sensitivity of the 2-dimensional manual analysis is significantly worse than that of our method.

TABLE 2
Average Percentage Variation in Influx Constant and Ratio Values Across All 8 Values of All 49 Cases with Varying Striatum ROI Position

	Shift (mm)			
	±2		±4	
Direction	K_i^c	$R_{s\text{-}to\text{-}c}$	K_i^c	$R_{s\text{-}to\text{-}c}$
L-R	4.7	3.0	10.3	6.8
A-P	2.2	2.0	5.6	4.0
S-I	2.1	1.0	4.4	2.5

Calculation of ROI Indicator Value

An experiment was also performed to ascertain the sensitivity of the influx constant to the proportion of striatum and cerebellum voxels used in calculations. This sensitivity was measured by computing, across all regions of all patients, the distribution of K_i^c obtained using different proportions of ROI voxels (Fig. 4). This plot indicated that as the used proportion of the striatum increased, the median K_i^c and $R_{s\text{-}to\text{-}c}$ values decreased, as did the maximum and both upper and lower quartiles. The plot also indicated that the minimum K_i^c value increased slightly with the proportion of voxels used, whereas the minimum $R_{s\text{-}to\text{-}c}$ values decreased slightly. Similar plots (not shown) were obtained for the other cerebellum proportions (25%, 75%, and 100%).

Comparison of Ratio and Influx Constant Values

Throughout the experiments, the $R_{s\text{-}to\text{-}c}$ computed from the final frame correlated best with K_i^c; therefore, all results described in the remaining experiments used the final frame for the static analysis. The highest correlation between K_i^c and $R_{s\text{-}to\text{-}c}$ values ($r^2 = 0.91$, $P < 0.0001$, for all regions considered together) was achieved using 25% of the brightest voxels in the cerebellum and 40% of the brightest voxels in the striatum (Fig. 5).

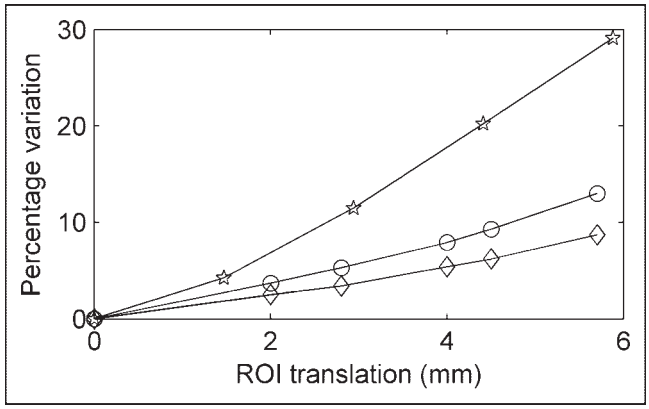

FIGURE 3. Variations of K_i^c values obtained from 3-dimensional ROIs (○), ratios obtained from 3-dimensional ROIs (◇), and K_i^c values obtained using 2-dimensional manual ROIs (☆).

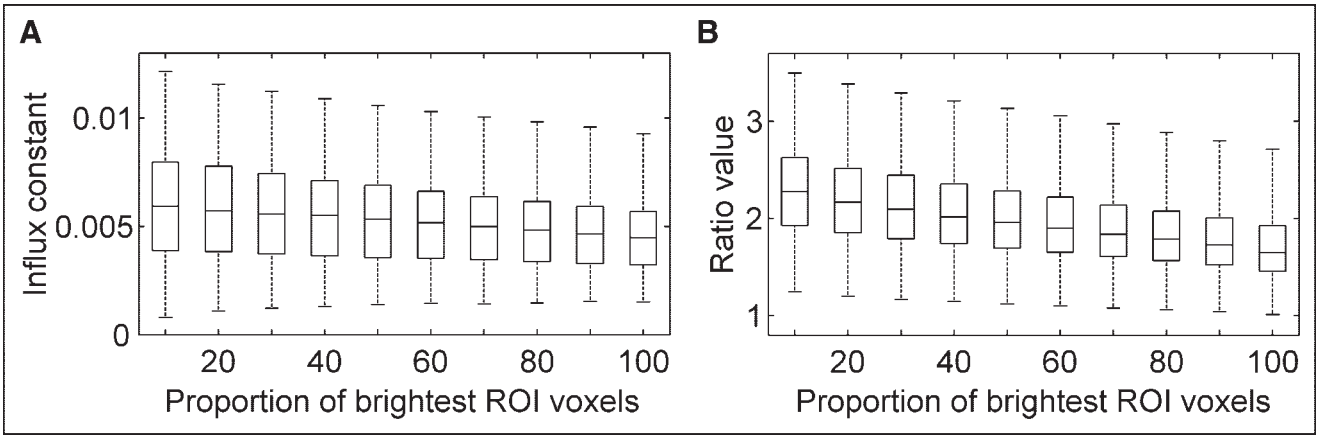

FIGURE 4. Box-and-whisker plot showing range of K_i^c values (A) and $R_{s\text{-}to\text{-}c}$ values (B) for different striatum proportions (using 50% of cerebellum voxels). Boxes indicate lower and upper quartiles and median.

However, plotting the correlation (r^2) against the proportion of cerebellum and striatum (Fig. 6) illustrates that although these particular values gave the highest correlation (by a small amount), correlations of $r^2 > 0.9$ were obtained with all striatum proportions between 20% and 80% when using either 25% or 50% of the cerebellum, and even the lowest correlation ($r^2 > 0.80$; obtained when using 100% of the cerebellum and 10% of the striatum) was still significant, at $P < 0.0001$.

The correlations obtained when each region was considered separately (Table 3) show that the putamen values had a stronger correlation than the caudate values. Plotting the lines of best fit for each of our 8 regions separately (Fig. 5A) showed that the relationships between $R_{s\text{-}to\text{-}c}$ and K_i^c for all putamen regions were similar; therefore, we grouped all points in these regions together (Fig. 5B), giving the single correlation $r^2 = 0.95$ ($P < 0.0001$). The correlations for the left and right caudate regions were slightly lower, and the lines of best fit were less similar. We believe the reason was the lower spread of values we had for uptake in the caudate. Grouping left and right regions together gave us a single correlation of $r^2 = 0.86$ ($P < 0.0001$) (Fig. 5B).

DISCUSSION

Motion Correction

The large range of percentage variation in K_i^c and the high SD suggest that the effect of patient movement during the acquisition can be highly significant. The small mean indicates that there is little bias, and thus values with motion correction appear randomly larger or smaller than those without. We contend, therefore, that it is important to correct for such motion before analysis, not least in order to enable reliable estimation of influx constants. This effect is likely to be more pronounced for smaller ROIs, because even slight patient movement could cause a large misalignment between corresponding ROIs in different frames.

Calculation of ROI Indicator Value

We had 2 key motivations for our choice of method for computing an indicator value for each ROI. Our first motivation was to account for the heterogeneous nature of the uptake values within each ROI. Our second motivation was that the anatomic ROIs, particularly the cerebellum, were significantly larger than the corresponding functional regions visible on the PET scans. The fact that the value of K_i^c

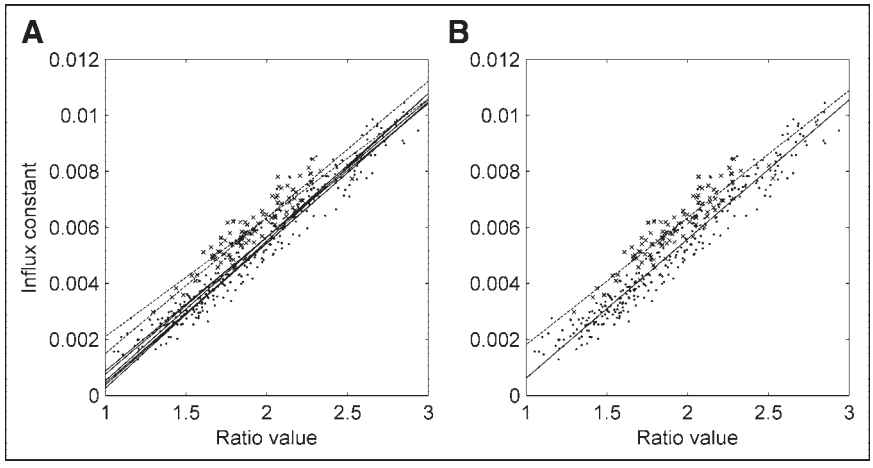

FIGURE 5. Correlation (r^2) between $R_{s\text{-}to\text{-}c}$ values and K_i^c values: both plots show the same 8 regions of all 49 cases (caudate as crosses, putamen regions as dots), with the best-fit lines relating the static and dynamic values in (A) shown for each region separately (caudate dashed, putamen solid); (B) shows the same data except that the best-fit lines are computed for left and right caudate regions together (dashed) and all 6 putamen regions (left and right) combined (solid).

decreased as the proportion of voxels increased (Fig. 4) suggests that as the proportion of voxels included in computations is increased, more low-intensity voxels are included, decreasing the indicator value for the ROI. This reduction is indistinguishable from reduced uptake, and hence the observed K_i^c is lower. Although the minimum K_i^c value increased with the proportion of striatum used, the quality of fit of the straight line in the Patlak graphical method was not uniform (data not shown); in particular, although fewer than 4% of our K_i^c values had an r value of less than 0.8, in all these cases K_i^c values were less than 0.003 (i.e., at the bottom of our range of K_i^c results). This finding suggests that the reason for the increasing minimum value of K_i^c with striatum proportion could be poor Patlak graphical fitting for low K_i^c values. The results of the ratio method behaved as expected for these low values.

Sensitivity of Values to ROI Placement

The small variation of the influx constant and ratio while one is perturbing the location of the cerebellum ROI indicates that the method described in this paper tolerates the misalignment of the cerebellum ROI to a comfortable extent (no more than 3.5% change in K_i^c for a 6-mm translation). When one is translating striatum ROIs, the variation of the influx constant and ratio is greater in the L-R direction than in the A-P and S-I directions because of the long, thin shape of the striatum: misalignment in the L-R direction more quickly moves the ROI outside the striatum. When compared with a 2-dimensional manual ROI method, the variation of influx constant is considerably smaller using the 3-dimensional method (Fig. 3), indicating an improved robustness by a factor of 2–3 from the 2-dimensional method outlined in this paper. The variation of ratio value is of a similar order of magnitude to the variation of influx constant, although it does appear to be slightly more robust, perhaps because of the simplicity of the method (e.g., because only a single time frame is considered, any motion artifacts remaining after motion correction are minimized).

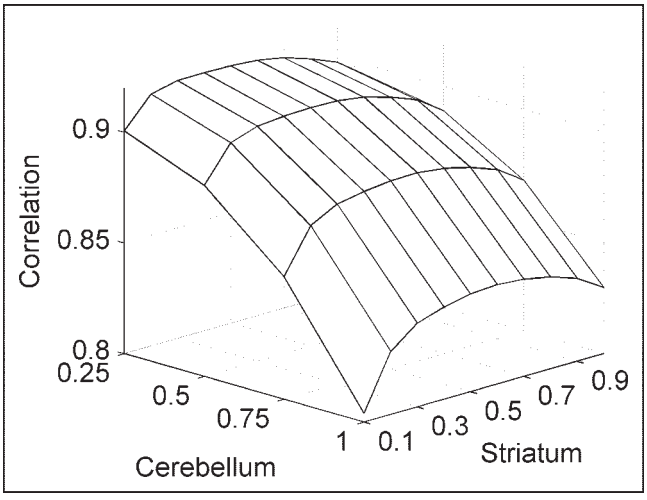

FIGURE 6. Variation in correlation between Patlak and static analysis values with different proportions of voxels from cerebellum and striatum.

TABLE 3
Correlation (r^2) Obtained for Each ROI Separately Using 25% of the Brightest Voxels from the Cerebellum and 40% of the Brightest Voxels from Each Striatal Region (All with $P < 0.0001$)

Region	Left	Right
Caudate	0.83	0.88
Putamen (rostral)	0.95	0.95
Putamen (mid)	0.95	0.96
Putamen (caudal)	0.91	0.92

Correlation Between Ratio and Influx Constant

It would be beneficial to be able to analyze FDOPA scans using just a short, static analysis rather than the full dynamic analysis. This ability would be clinically preferable because the time spent in the scanner by the patient is shorter (e.g., 20 min rather than 2 h). Also, multiple patients could be scanned in the time required for a single dynamic scan. A good correlation was obtained between influx constants and ratios using a 2-dimensional slab of data with standard elliptic ROIs ($r^2 = 0.92$ for putamen and $r^2 = 0.75$ for caudate, $P < 0.0001$) when a 10-min scan was used with a postinjection delay of 95 min (*6*) (compared with the final frame). Our results agree with those findings, in that the final frame in our acquisition gave the highest correlation between ratio and K_i^c values. Note, however, that in that study, the scores (both ratio and influx constant) obtained from left and right regions were averaged. We believe that this averaging reduces the sensitivity of the analysis, and we have elected to distinguish the results for left and right striata, allowing possible further analysis based on the bilateral progression of PD, a point mentioned by Rakshi et al. (*23*).

CONCLUSION

Our techniques for motion correction, ROI delineation, and ROI indicator value extraction were effective and robust for analyzing FDOPA scans (these techniques are not limited to FDOPA or PD and should also be applicable to similar analyses of other dynamic or static scans). The motion correction was proven important for getting reliable values from dynamic scans. The experiments showed that by using standard normalized volumetric ROIs and a systematic way of placing them, our analysis techniques were less sensitive (by a factor of 2–3) to ROI position than in a more typical 2-dimensional analysis and that the ratios obtained were slightly less sensitive to ROI position than were influx constants. We also found a good correlation between K_i^c and $R_{s\text{-}to\text{-}c}$ values, confirming the feasibility of using a short, patient-friendly static scan instead of a dynamic scan in FDOPA brain PET analysis for suspected PD. Our results suggest that a good correlation can be obtained

with little concern for the exact proportion of voxels used from each ROI to compute its indicator value, leaving the selection of this parameter to be based on other factors such as accommodating the difference in size between functional and anatomic cerebellum ROIs.

REFERENCES

1. Sethi KD. Clinical aspects of Parkinson disease. *Curr Opin Neurol.* 2002;15: 457–460.
2. Hughes AJ, Daniel SE, Kilford L, Lees AJ. Accuracy of clinical diagnosis of idiopathic Parkinson's disease: a clinico-pathological study of 100 cases. *J Neurol Neurosurg Psychiatry.* 1992;55:181–184.
3. Otsuka M, Ichiya Y, Kuwabara Y, et al. Differences in the reduced ^{18}F-Dopa uptakes of the caudate and the putamen in Parkinson's disease: correlations with the three main symptoms. *J Neurol Sci.* 1996;136:169–173.
4. Ravina B, Eidelberg D, Ahlskog JE, et al. The role of radiotracer imaging in Parkinson disease. *Neurology.* 2005;64:208–215.
5. Doudet DJ, Miyake H, Finn RT, et al. 6-^{18}F-L-dopa imaging of the dopamine neostriatal system in normal and clinically normal MPTP-treated rhesus monkeys. *Exp Brain Res.* 1989;78:69–80.
6. Dhawan V, Ma Y, Pillai V, et al. Comparative analysis of striatal FDOPA uptake in Parkinson's disease: ratio method versus graphical approach. *J Nucl Med.* 2002;43:1324–1330.
7. Hoshi H, Kuwabara H, Leger G, Cumming P, Guttman M, Gjedde A. 6-[^{18}F]fluoro-L-dopa metabolism in living human brain: a comparison of six analytical methods. *J Cereb Blood Flow Metab.* 1993;13:57–69.
8. Patlak CS, Blasberg RG, Fenstermacher JD. Graphical evaluation of blood-to-brain transfer constants from multiple-time uptake data. *J Cereb Blood Flow Metab.* 1983;3:1–7.
9. Patlak CS, Blasberg RG. Graphical evaluation of blood-to-brain transfer constants from multiple-time uptake data: generalizations. *J Cereb Blood Flow Metab.* 1985;5:584–590.
10. Vingerhoets FJ, Schulzer M, Ruth TJ, Holden JE, Snow BJ. Reproducibility and discriminating ability of fluorine-18–6-fluoro-L-Dopa PET in Parkinson's disease. *J Nucl Med.* 1996;37:421–426.
11. Huang SC, Yu DC, Barrio JR, et al. Kinetics and modeling of L-6-[^{18}F]fluoro-dopa in human positron emission tomographic studies. *J Cereb Blood Flow Metab.* 1991;11:898–913.
12. Shoghi-Jadid K, Huang SC, Stout DB, et al. Striatal kinetic modeling of FDOPA with a cerebellar-derived constraint on the distribution of volume of 30MFD: a PET investigation using non-human primates. *J Cereb Blood Flow Metab.* 2000;20:1134–1148.
13. Cumming P, Kuwabara H, Gjedde A. A kinetic analysis of 6-[^{18}F]fluoro-L-dihydroxyphenylalanine metabolism in the rat. *J Neurochem.* 1994;63:1675–1682.
14. Phelps ME. *PET: Molecular Imaging and Its Biological Applications.* New York, NY: Springer; 2004:509–583.
15. Whone AL, Bailey DL, Remy P, Pavese N, Brooks DJ. A technique for standardized central analysis of 6-(18)F-fluoro-L-DOPA PET data from a multicenter study. *J Nucl Med.* 2004;45:1135–1145.
16. Yu DC, Huang SC, Grafton ST, et al. Methods for improving quantitation of putamen uptake constant of FDOPA in PET studies. *J Nucl Med.* 1993;34:679–688.
17. Andersson JL. How to obtain high-accuracy image registration: application to movement correction of dynamic positron emission tomography data. *Eur J Nucl Med.* 1998;25:575–586.
18. Tzourio-Mazoyer N, Landeau B, Papathanassiou D, et al. Automated anatomical labeling of activations in SPM using a macroscopic anatomical parcellation of the MNI MRI single-subject brain. *Neuroimage.* 2002;15:273–289.
19. Finlay BL, Darlington RB. Linked regularities in the development and evolution of mammalian brains. *Science.* 1995;268:1578–1584.
20. Morrish PK, Sawle GV, Brooks DJ. Regional changes in [^{18}F]dopa metabolism in the striatum in Parkinson's disease. *Brain.* 1996;119:2097–2103.
21. Rousset OG, Deep P, Kuwabara H, Evans AC, Gjedde AH, Cumming P. Effect of partial volume correction on estimates of the influx and cerebral metabolism of 6-[(18)F]fluoro-L-dopa studied with PET in normal control and Parkinson's disease subjects. *Synapse.* 2000;37:81–89.
22. Rottenberg DA, Moeller JR, Strother SC, Dhawan V, Sergi ML. Effects of percent thresholding on the extraction of [^{18}F]fluorodeoxyglucose positron emission tomographic region-of-interest data. *J Cereb Blood Flow Metab.* 1991;11: A83–A88.
23. Rakshi JS, Uema T, Ito K, et al. Frontal, midbrain and striatal dopaminergic function in early and advanced Parkinson's disease: a 3D [(18)F]dopa-PET study. *Brain.* 1999;122:1637–1650.